Special Issue: DTD 2006 in JAPAN
Original Article
J. Jpn. Soc. Microgravity Appl. Vol. 24 No. 3 2007 (235-240)

The Opposed-Flow Flame Spread over Thin Solid Fuel in Finite Space under Normal and Microgravity

Xia ZHANG

National Microgravity Laboratory, Institute of Mechanics, Chinese Academy of Sciences,
No.15 Beisihuanxi Road, Beijing, China (100080), zhangxia@imech.ac.cn

Abstract

Apparatus to simulate microgravity combustion under normal gravity is important for the fire safety of manned spaceflight. The narrow channel is such an apparatus in which the buoyant flow is restricted effectively. However, the comparability of flame spread in different gravities is still an open question. In present paper, the opposed-flow flame spread over thin solid fuel in finite space under different gravities was compared experimentally and numerically. The comparison of flame appearances and flame spread rates under various gravities suggest that the horizontal channel of 1 cm height can suppress natural convection effectively. Such apparatus can simulate the microgravity flame spread in the channel of same geometrical size. Therefore, using the horizontal narrow channel on the ground to simulate the microgravity flame spread in the same environment, then considering the effect of channel size on flow field and heat loss to get the characteristics of microgravity flame spread in space of other size may be a feasible method.

Keywords: microgravity, flame spread, thin solid fuel, finite space, numerical simulation, experiment

1. Introduction

The flame spread over solid surface is a classical problem in combustion science owing to its importance in fire safety in both ground and manned spacecraft. Eliminating potential fuels out of the materials is the basic method to protect spacecraft from fire. The criterion of materials screening is their flammability[1]. Since gas flow speed has strong effect on flame spread, the combustion behaviors of materials in normal and microgravity will be obviously different due to their contrast of natural convection. To evaluate the flammability of materials used in the manned spacecraft, tests should be performed under microgravity. Nevertheless, the cost is high, so apparatus to simulate microgravity combustion under normal gravity was developed. The narrow channel is such an apparatus in which the buoyant flow is restricted effectively[2, 3]. The experimental result of the horizontal narrow channel is consistent qualitatively with that of Mir Space Station. Quantitatively, there still is obvious difference. However, the comparability of flame spread in different gravities is still an open question. In present paper, the opposed-flow flame spread over thin solid fuel between different gravities was compared experimentally and numerically.

2. Experimental System and Method

The experimental configuration is shown in **Figure 1.** It mainly consists of a test section, a CCD Camera and a fan. The test section is a combustion channel with a length of 400 mm, a width of 200 mm and a variable height *h*. An aluminum frame to hold fuel occupies the center plan normal to the height of the channel. Two ends of the channel are filled with honeycomb to make gas flow uniform. A fan is installed near one of honeycombs to induce the gas flow in the range of 1-30 cm/s. The flow velocity is adjusted by the voltage imposed on the fan and the relation between the velocity and voltage is calibrated by using laser visualization techniques in advance. The fuel sample, thin paper with a thickness of 0.0245 mm and an area density of 17.0 g/m^2, is pasted on the sample holder. The paper is 200 mm long and 100 mm wide. The igniter is an electrical hot wire with cold resistance of 4 Ω. The sample is ignited at the downstream end by heating the wire electrically.

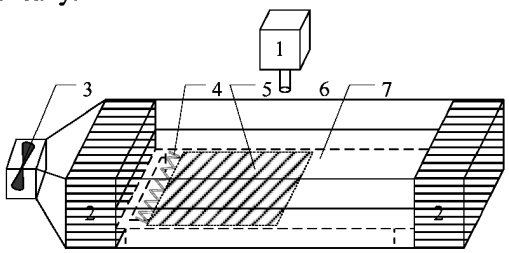

1. CCD Camera 2. Aluminium honeycomb 3. Fan 4. Igniter 5. Sample 6. Combustion channel 7 Sample holder

Fig.1 The experimental configuration

The experiment is performed in the air of 1 atm under both normal and microgravity. Under normal gravity, the experiment starts with the run of fan. As the fan has run for 15 s and the induced flow gets into steady state, the igniter is heated by imposing 24 V voltage for 5 s so that the fuel is ignited. The flame spread is recorded with a color CCD camera of 12 mm focus. The flame spread rate can be computed according to the displacement of flame front with the time during the steady flame spread.

The microgravity condition is achieved in the 3.6 s drop tower of National Microgravity Laboratory, Chinese Academy of Sciences, Beijing. The

experimental apparatus was closed in a single capsule before microgravity test is performed. The microgravity level has not been measured accurately but estimation implies that the level is about 10^{-3} g_e, where g_e is gravitational acceleration on the ground. The procedure of microgravity experiment is approximately same with that of normal gravity. However, the drop capsule is released when the fuel has been ignited for 5 s. In addition, the flame spread rate is computed according to the displacement of flame front with the time when the capsule enters into free fall condition and the variation of the flame appearance stops.

The experiment is carried out in the channel placed horizontally and vertically in normal gravity with gravitational acceleration against the forced gas flow and normal to the fuel surface, and vertically in microgravity with residue gravitational acceleration against the forced gas flow. Hence, the opposed-flow flame spread in the downward, horizontal direction under normal gravity and in the downward direction under microgravity is carried out.

3. Mathematical Model

The configuration of two-dimensional opposed-flow flame spread over thin solid fuel in the flow channel is sketched in **Figure 2**. The oxidized gas flows into the channel with uniform inlet velocity u_0, while flame spreads upstream with rate u_f. The coordinate origin is set on the leading edge of the flame, which makes the flame spread a steady process. The x-coordinate, along the fuel surface, is 40 cm long with 25 cm upstream and 15 cm downstream. The y-coordinate, normal to the fuel surface, is the channel height to vary. The simulation is performed on the configurations which is similar to the experimental cases, i.e., the configurations placed horizontally and vertically in normal gravity with gravitational acceleration g_e against y-coordinate and x-coordinate, and vertically in microgravity with gravitational acceleration of 10^{-3} g_e against x-coordinate. Hence, the opposed-flow flame spread in the downward, horizontal direction under normal direction and in the downward direction under microgravity is simulated.

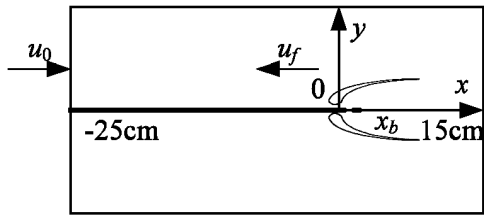

Fig.2 Opposed-flow flame spread over thin solid fuel

The flame spread model contains gas and solid phase model. The gas phase model consists of two-dimensional partial differential equations for the conservation of mass, momentum, species and energy. The combustion of gas phase is treated as nonreversible, one-step, second order, finite rate Arrhenius reaction. The solid phase model comprises the ordinary differential equations for the conservation of mass and energy. The pyrolysis of fuel is taken as nonreversible, one-step, first order, finite rate Arrhenius reaction. Since the fuel is thin enough, it is considered to share the same plane with the middle section of the channel. In the simulation, gas phase radiation is ignored, but solid radiation is considered. The gas and solid phase models are coupled together through boundary conditions at the interface. The flame spread rate u_f consists in equations as an eigenvalue.

The solid fuel is the cellulose paper with chemical formula of $C_6H_{10}O_5$. In the simulation, the thickness of fuel is assumed to keep unchanged, but the density of the fuel is decreased until pyrolysis stops.

The universal form of the gas phase equations for flame spread is

$$\frac{\partial}{\partial x}(\rho u\phi)+\frac{\partial}{\partial y}(\rho v\phi)=\frac{\partial}{\partial x}(\Gamma_\phi\frac{\partial\phi}{\partial x})+\frac{\partial}{\partial y}(\Gamma_\phi\frac{\partial\phi}{\partial y})+S_\phi, \quad (1)$$

where the meanings of ϕ, Γ_ϕ and S_ϕ are shown in **Table 1**.

Table 1 The meanings of ϕ, Γ_ϕ and S_ϕ in Equation(1)

Equation	ϕ	Γ_ϕ	S_ϕ
Mass	1	0	0
x coordinate momentum	u	μ	$-\frac{\partial p}{\partial x}+(\rho_\infty-\rho)g_x$
y coordinate momentum	v	μ	$-\frac{\partial p}{\partial y}+(\rho_\infty-\rho)g_y$
Energy	T	μ/Pr	$-\Delta H\varpi/C_g$
Species	Y_i	μ/Sc	$s_i\varpi$

In Table 1, the symbols ρ, u, v, p, T and Y_i are gas density、x and y coordinate velocity components, pressure, temperature and mass fraction of species i respectively. i denotes fuel, oxygen, nitrogen, vapour and carbon dioxide respectively. μ、Pr and Sc are viscosity, Prandtl number and Schmidt number respectively. C_g, g, ΔH, ω and s are specific heat capacity, gravitational acceleration, reaction heat, reaction rate and stoichiometric mass ratio of species i respectively.

The chemical reaction of fuel gas (cellulose) and oxygen is

$$C_6H_{10}O_5+6O_2=6CO_2+5H_2O. \quad (2)$$

The reaction rate $\varpi=B_g\rho^2Y_fY_oe^{-E_g/RT}$, where B_g, E_g and R are pre-exponential factor, activation energy and universal gas constant respectively.

The boundary conditions of gas phase equations are as follows:

at $x=-\infty$ (inlet),

$u = u_0 + u_f$, $v = 0$, $T = T_0$,

$Y_i = Y_{i0} (i = \mathrm{F}, \mathrm{O}_2, \mathrm{N}_2, \mathrm{H}_2\mathrm{O}, \mathrm{CO}_2)$, (3)

at $x = \infty$ (outlet),

$\frac{\partial \phi}{\partial x} = 0 \ (\phi = u, v, T, Y_i (i = \mathrm{F}, \mathrm{O}_2, \mathrm{N}_2, \mathrm{H}_2\mathrm{O}, \mathrm{CO}_2))$, (4)

at $y = 0$ and $y = y_\infty$ (wall),

$u = u_f$, $v = 0$, $T = T_0$,

$\frac{\partial Y_i}{\partial y} = 0 (i = \mathrm{F}, \mathrm{O}_2, \mathrm{N}_2, \mathrm{H}_2\mathrm{O}, \mathrm{CO}_2)$, (5)

at fresh solid fuel,

$u = u_f$, $v = v_w$, $T = T_s$, $D \frac{\partial Y_F}{\partial y} = m(Y_F - 1)$,

$D \frac{\partial Y_i}{\partial y} = m Y_i \ (i = \mathrm{O}_2, \mathrm{N}_2, \mathrm{H}_2\mathrm{O}, \mathrm{CO}_2)$, (6)

where $D = \frac{\mu}{Sc}$, m, v_w, T_s are mass diffusivity, mass flux of pyrolyzed products, fuel gas jet velocity at the fuel surface and solid surface temperature respectively, which are determined by the coupled equations of gas and solid phase.

The pyrolysis of solid fuel is the first order Arrhenius reaction[4], which is given by

$m = B_s \rho_s \tau e^{-E_s / RT_s} = \rho v_w$. (7)

The mass balance analysis for the solid fuel yields that

$m = \frac{d}{dx} (\rho_s \tau u_f)$, (8)

where B_s and E_s are pre-exponential factor and activation energy respectively, ρ_s and τ are density and thickness of solid fuel respectively,

$B_s = B_{s0} \left(\frac{\rho_s}{\rho_{s0}} \right)^{0.8}$ (9)

where B_{s0} and ρ_{s0} are the referenced value of pre-exponential factor and initial density respectively.

Neglecting the heat conduction inside the solid, the energy balance of thin solid is expressed as

$q_c - q_r = \rho_s \tau u_f C_s \frac{dT_s}{dx} + m[L_v + (C_g - C_s)(T_s - T_0)]$, (10)

where q_c and q_r are the conductive and radiative heat fluxes respectively, L_v and C_s are latent heat of vaporization and specific heat of solid. The conductive heat flux q_c can be obtained from gas temperature field by

$q_c = \lambda \frac{\partial T}{\partial y}\Big|_{y=0}$. (11)

where λ is thermal conductivity of gas phase. The radiative heat flux is given by

$q_r = \varepsilon (T_s^4 - T_0^4)$, (12)

where ε is the solid thermal emissivity.

The boundary conditions for solid phase equations are

at $x = -\infty$, $T_s = T_{s0}$, $\rho_s = \rho_{s0}$. (13)

The property values are evaluated as follows. The gas density is determined according to the equation of state

$\rho = \frac{p}{RT} \sum_i \frac{Y_i}{M_i}$. (14)

The viscosity is dependent upon temperature in the form of power law, i.e.,

$\mu = \mu_0 \left(\frac{T}{T_0} \right)^{\frac{2}{3}}$. (15)

The gas phase specific heat is the function of temperature and composition.

$C_g = \sum_i Y_i C_{pi}(T)$, (16)

where C_{pi} is the specific heat of species, which is related with its temperature in polynomial form[5]. Other parameters used in the simulation are shown in **Table 2**.

Table 2 The property values

Symbol	Value	Source
T_0	300 K	-
Y_{O0}	23.3%	-
B_g	2.5×10^{12} m^3·kg^{-1}·s^{-1}	-
E_g	2.027×10^5 J·mol^{-1}	-
□H	1.674×10^7 J·kg^{-1}	[6]
Pr	0.7	-
Sc	0.7	-
ρ_{s0}	693.9 kg·m^{-3}	
τ	2.45×10^{-5} m	
C_s	1256 J·kg^{-1}·K^{-1}	[6]
B_{s0}	2.0×10^{17} s^{-1}	[4]
E_s	2.2×10^5 J·mol^{-1}	[4]
L_v	5.7×10^5 J·kg^{-1}	[4]
ε	0.92	[7]

Since the full model comprises gas and solid phase model, the coupled method is used to obtain solution. The gas phase equations is solved using SIMPLEC algorithm[8], in which velocities are arranged at staggered meshes. The discretization equations given by finite volume method are solved using the line-by-line scanning method incorporating with TDMA (tri-diagonal matrix algorithm). The solid pyrolysis equations are solved using fourth order Runge-Kutta method. The nonuniform grid with the minimum and maximum cell size of 0.1 mm and 1 mm is used. The cell near the leading edge of flame, solid surface and channel wall is most fine. The x-grid is expanded upstream and downstream with the ratio of 1.05 from the leading edge of flame. The y-grid is expanded until it reaches the middle plane between the solid fuel and channel wall, before it contracts. The ratio for both expansion and contraction is 1.05. For the channel with half height of 20 mm, the computational region 400 mm × 20 mm is divided into 460 × 106 cells.

4. Results and Discussion

The top view photos of the flame in the channel of various heights in different spread directions under normal and microgravity are shown in **Figure 3**. Under microgravity, in the channel of 1 cm height, the flame in the forced gas flow of 3 cm/s breaks into several yellow flamelets, due to the lack of the oxygen. As the forced gas flow increases (4.5 and 6 cm/s), the flame front becomes continuous with lower flame temperature, which is implied by the color of the flame. In the range of forced gas flow of 3-6 cm/s, the flame has length of only about 0.5 cm. As the forced gas flow increases to 9 cm/s, the flame becomes hotter and longer. In the horizontal channel of 1 cm height, when the forced gas flow is in the range of 3-4.5 cm/s, the flame also breaks into flamlets. As the forced gas flow reaches 6 cm/s, the flame front presents continuous form. The color and length of the flame in horizontal channel is similar to that of microgravity condition. In the vertical channel of 1 cm height, when the forced gas flow is low, i.e., 3-4.5 cm/s, the flame does not break into flamlets, however, part of the fuel is not burnt. As the gas flow reaches 6 cm/s, the fuel will burn completely. The color of the flame in vertical channel is bright yellow, and the length of the flame is about 1-2 cm. These two aspects are totally different with those of the flame in channel under microgravity or being horizontally placed. As the height of channel increases (h=2 cm), in channels both being horizontally and vertically placed, the flame becomes hotter and the flame length becomes longer. The reason is that in channels of larger height, the heat loss is lower and the suppression of natural convection is relaxed.

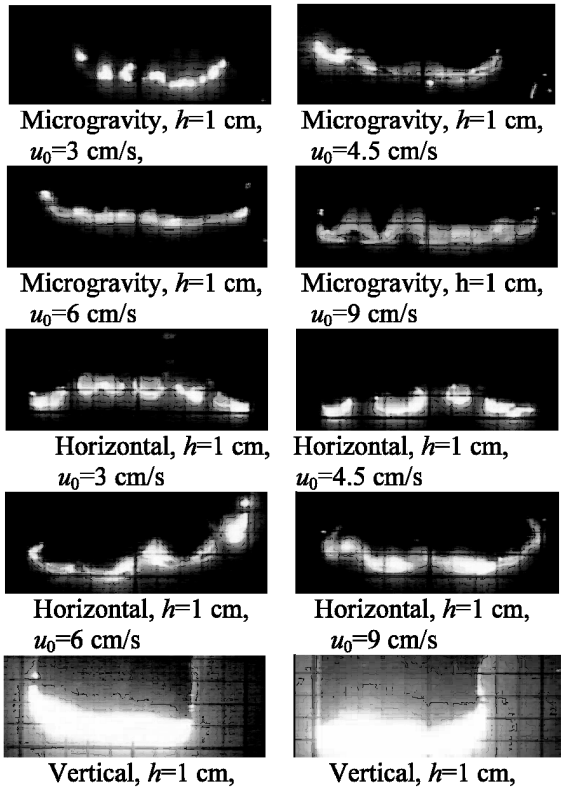

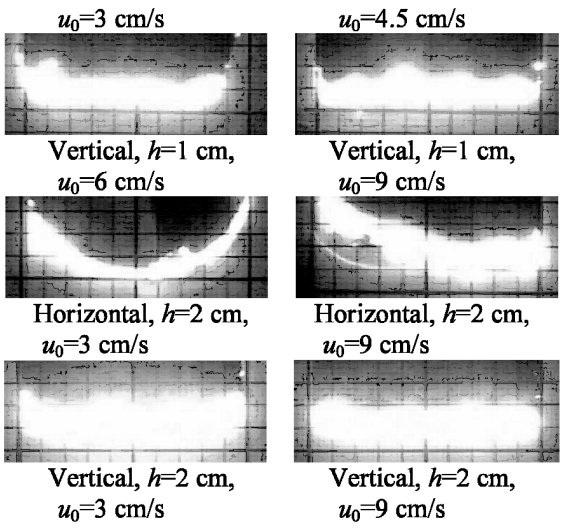

Fig.3 The top view photos of flame under various spread directions

From the view of flame appearance, the flame in horizontal channel of 1 cm height rather than other channel has comparability with that under microgravity. The rupture of flame front under low speed forced gas flow implies that there is a lower limit of gas flow for two-dimensional flame spread, which may be caused by the oxygen lack. However, under this limit, flame may not quench. Instead, it can exist in the form of flamelets so that side diffusion of oxygen can occur. This phenomenon is important for the fire safety of manned spacecraft.

The variation of flame spread rate with forced gas flow speed for various spread directions and different sizes of channel is shown in **Figure 4**. For the convenience of comparison, the result of microgravity experiment in large space is also given. In channels of 1cm height, the spread rate of horizontal flame and flame under microgravity increases as forced flow speed increases. This is in agreement with the experimental result given by larger test section[9]. However, the flame spread rate in small and large test sections is obviously different, since both of the flow and heat conditions are different. Under low speed forced gas flow, the flame in the channel of 1 cm height spreads in almost the same rate as that in microgravity, since both of the flow and heat conditions for the two cases are similar. This shows that the horizontal narrow channel can restrict natural convection. In vertical channel of 1 or 2 cm height, or horizontal channel of 2 cm height, the flame spread rate almost does not depend on the low speed forced gas flow, because the flame spread is mainly controlled by the natural convection. This is entirely different from the result of microgravity and shows that the horizontal channel with larger height and vertical channel can not restrict natural convection. For horizontal channel, the channel of 1 cm height (The Grashof number is 149 as the half height is taken as the characteristic length), is the

apparatus to restrict natural convection in flame spread process.

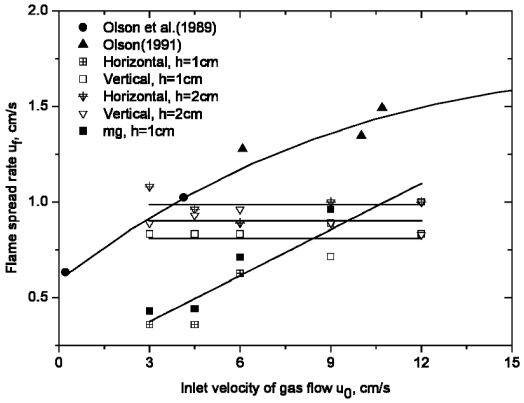

Fig.4 The variation of flame spread rate as the function of gas flow speed in air

Under lower speed forced gas flow, the effect of buoyancy on flame spread is more obvious. For forced gas flow of 5 cm/s, the numerical results of the effects of gravity on the temperature and velocity field near the flame in channels of 1 cm height are shown in **Figure 5**. The flame shape and flow and temperature field near the flame is similar for different gravities. The flame spreading in horizontal direction is symmetrical. However, far from the flame, the flame spreading vertically downward has a weak reversed flow zone near the wall, and flame spreading horizontally has asymmetrical velocity and temperature profile, which is different from the case of microgravity. Since it is the flame front that control opposed-flow flame spread, and downstream has little influence, the characteristics of flames in channel of 1 cm height under different gravities will exhibit no distinct difference. This is in agreement with the experiment results.

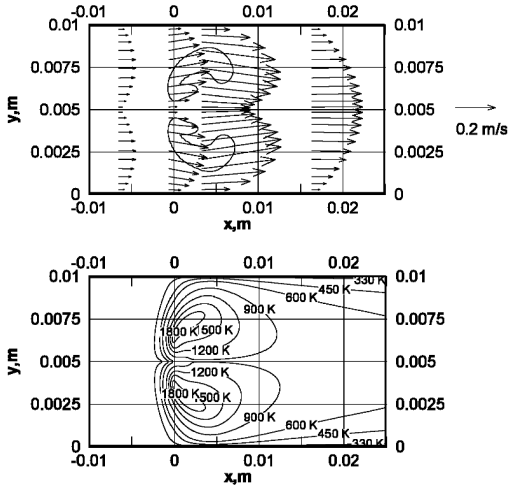

a) Microgravity

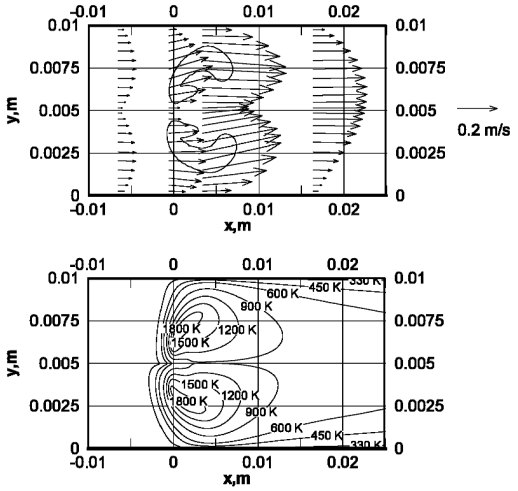

b) Horizontal

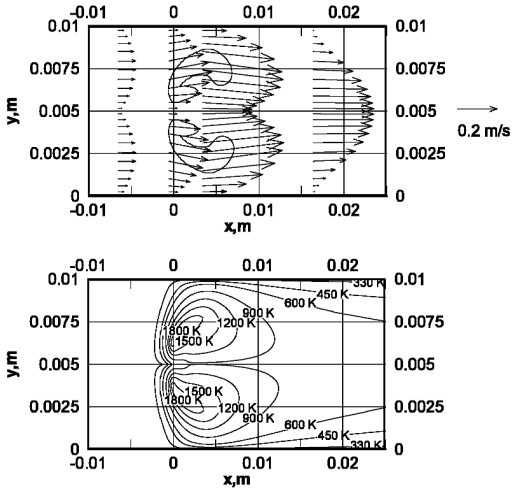

c) Vertical

Fig.5 The numerical results of temperature and velocity profiles near the flame in different spread directions in the channel of 1 cm height (u_0= 5 cm/s)

The numerical result of flame spread rate in narrow channel under different gravities as the function of gas flow speed is shown in **Figure 6**. Since the cost of numerical simulation is much lower compared with that of experiment, the results for a wider velocity range are given. Evidently, for the channel of 1 cm height, the flame spread rate in different directions has little difference. The reason is that the buoyant convection can be ignored for both normal and microgravity, since the Grashof number is small enough although still different. However, compared with the downward spread flame, the horizontal spread flame simulates the flame under microgravity better. For the channel of 2 cm height, both the downward and horizontal spread flame appears obviously different with microgravity flame. The downward flame spread rate is less, while the horizontal rate is greater, than microgravity rate. This is the result of residue natural convection. For downward spread flame, the mixed convection makes the flame enter into blow off branch, so the flame spread becomes slowly. For horizontal spread flame,

the natural convection makes one part of flame opposed-flow flame while the other part wind-aided flame, this feature is significant under low speed forced gas flow. Due to the increase of residue natural convection, the difference between flame spreads in different directions becomes more obvious as the height of channel increases. From the aspect of flame spread rate, the horizontal channel of 1 cm height can suppress the natural convection effectively.

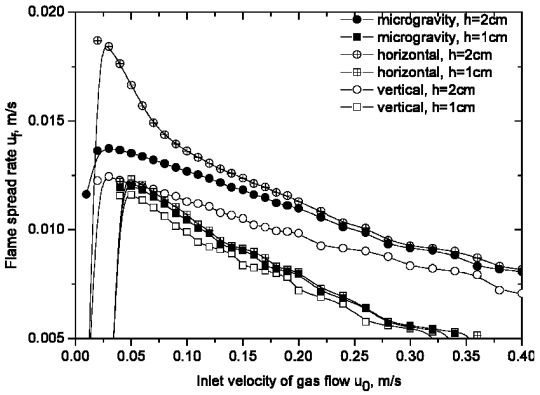

Fig. 6 The numerical result of flame spread rate in narrow channel in different directions

The variation of the channel height must influence the flow field in the channel and heat loss at the wall, and hence the flame spread. Therefore, the flame spread under the same gravity condition but in channels with different geometrical size will be totally different. Similarly, to simulate the microgravity combustion in large space by using the small size test section on ground will not give good result. This is why references[2, 3] can only get result with qualitatively satisfaction. However, in narrow channel, the Grashof numbers in flame spread under microgravity and normal gravity is still different, but the they are so small that the residue natural convection can be ignored. Therefore, the flame spread in narrow channel under different gravities is similar. Because of this, using the horizontal narrow channel on the ground to simulate the flame spread in the same environment under microgravity, then considering the effect of channel size on flow field and heat loss to get the characteristics of flame spread under microgravity in space of other size may be a feasible method.

Since the gas phase radiation is ignored, and over simplified chemical reaction mechanism is used in simulation, the result is not precise quantitatively. However, this does not influence the qualitative conclusions drawn in the paper.

5. Summary

The opposed-flow flame spread over the thin solid fuel in finite space under normal and microgravity was studied experimentally and numerically. The comparison of flame appearances and flame spread rates under different gravities suggest that the horizontal channel of 1 cm height can suppress natural convection effectively. Such apparatus can be used to simulate the microgravity flame spread in the channel of same geometrical size. Therefore, using the horizontal narrow channel on the ground to simulate the flame spread in the same environment under microgravity, then considering the effect of channel size on flow field and heat loss to get the characteristics of flame spread under microgravity in space of other size may be a feasible method.

Acknowledgments

The author thanks Engineer Jian YU of Beijing MacroSpace Co. Ltd. for the help on the laser visualization techniques.

References

1) NASA Technical Standard, "Flammability, Odor, Offgassing, and Compatibility Requirements and Test Procedures for Materials in Environments That Support Combustion", NASA STD-6001, 1998.
2) Ivanov, A. V., Balashov, Ye. V., Andreeva, T. V., and et al., "Experimental Verification of Material Flammability in Space", NASA CR-1999-209405, 1999.
3) Melikhov, A. S., Bolodyan, I. A., Potyakin, V. I., and et al., "The study of polymer material combustion in simulated microgravity by physical modeling method", In: Sacksteder K, ed, "Fifth Int Microgravity Comb Workshop", NASA CP-1999-208917, 1999, 361.
4) Kashiwagi, T., Nambu, H., *Comb Flame*, **88**, 345, 1992.
5) McBride, B. J., Zehe, M. J., Gordon, S. "NASA Glenn Coefficients for Calculating Thermodynamic Properties of Individual Species", NASA TP-2002-211556, 2002.
6) Frey, Jr. A. E., T'ien, J. S., *Comb Flame*, **36**, 263, 1979.
7) Hottel, H. C., Sarofim, A. F., "Radiative Transfer", McGraw-Hill, 1967.
8) Van Doormaal, J. P., Raithby, G. D., *Numerical Heat Transfer*, **7**, 147, 1984.
9) Olson, S. L., *Comb Sci Tech*, **76**, 233, 1991.

Received October 25, 2006
Accepted for publication, February 4, 2007